Authors' response to reviewer #1 comments on OS-2019-34-R1

Authors' response to the individual comments is denoted in red

Report 1

First, I want to thank the authors for their response to my previous comments. Overall, the authors have suitably addressed my comments and clarified the points I raised. While I still think that this paper is largely an academic exercise, it is scientifically valid (assuming the analysis has been properly done), and so it is not my place to hold this paper up. I have only one remaining important comment and a few minor ones.

The authors dismiss my comment about the arbitrariness of the metric used to assess the accuracy of the various detection methods by saying that "Indeed, our choice is arbitrary but so is any other choice". The authors' response is rather unscientific and I disagree with it. Choices about skill metrics should be governed by logical rather than arbitrary considerations and they should be clearly justified, otherwise the results will be suspect. On a related comment, I think that rather than saying whether or not a method detects the true propagation speed based on an arbitrary metric, it would be far more useful to provide a measure of the uncertainty associated with estimates of propagation speed.

We consider another scoring "yardstick": 1 at the bin, 2/3 at the nearest neighbors, 1/3 at the next to nearest neighbors and 0 away. The statistics of success of the 4 methods differs only slightly (up to 3%) from the "yardstick" we originally employed (which was 1/2, 1, 1/2). Despite the statistical (perhaps even somewhat arbitrary) of our examination it underscores the unreliable nature of the currently employed methods in detecting the phase speed of actual/observed signals.

The authors write "Indeed, our choice is arbitrary but so is any other choice. We will emphasize it in the revised text.". However, I cannot see where this has been emphasized in the text.

Right, the issue is addressed in the revised version (see L. 14-16 on P. 4 and L. 10-11 on P. 5)

Similarly, the authors write "As for the number of realizations, we didn't find significant difference between 25, 50 or 100 repeats." This is not mentioned in the paper and I think it should.

The issue is addressed in the revised version where 25 and 100 were added to the original repeats of 50 (see L. 9 on P. 5)

Authors' response to reviewer #2 comments on OS-2019-34-R1

Authors' response to the individual comments is denoted in red

Report 2
I rather struggle to see the point of this paper; it seems to be setting up an implausible strawman problem and then shooting it down.

The sermon of this paper is that no currently employed method (and we examine more than just the Radon method) can be considered reliable in detecting the correct phase speeds of observed signals in the ocean. To establish the inaccuracy of these methods we use artificial signals with known phase speeds that mimic in some general way (more than 1 amplitude and many phase speeds) oceanic signals. There is no "strawman" in our problem – just an artificial signal that examines whether these methods can detect the known phase speed in an artificially generated "signal". If the reviewer knows of a more fitting test s/he should have pointed it to the community since as it now stands the reviewer's approach does not permit any examination of a proposed method (in any field!) since, by definition, such an examination implies the application of a known speed to an artificial signal in order test the detection accuracy of the method being examined.

The idea behind the radon transform is that, in situations where there is a dominant propagation speed, it identifies that speed as a direction in t-x space along which the variance of the mean signal is maximised. The emphasis is on "dominant speed". This requires that there be either a single mode propagating at that speed with squared amplitude larger than the sum of the squares of the amplitudes of all other modes, or that there be a cluster of modes with similar speeds sufficient to be dominant over the modes with different speeds. The former case clearly requires the single mode to have a much larger amplitude than all the other modes. That seems to be what this paper is showing (also from Figure 5, we see how the "random" choice of speeds for other modes will tend to produce a clustering of energy at slower speeds: the result will depend on how the randomly chosen modes happen to cluster as a function of theta, with different choices giving different results).

The reviewer might be right in suggesting that when "a single mode propagating at that speed with squared amplitude larger than the sum of the squares of the amplitudes of all other modes" there is a dominant mode (as shown in our Fig. 3b for N=20 and amplitude of 5 for the dominant input mode so $5^2 = 25 > 19 \times 1$). However, in the real ocean it is impossible to determine the relevant amplitudes and the number of modes (N).

The "cluster of modes with similar speeds" the reviewer seeks is represented in our study by the width of the bin i.e. all modes in each bin are assumed to have the same amplitude. The addition of internal amplitude structure in each bin will not change the statistics we compute.

It is hard to think of a physical system for which this extreme case is a plausible model. If there is propagation, there is likely to be a smooth variation of speeds as a function of frequency and wavenumber. The aim with radon transforms as applied to Rossby waves is usually to identify the long Rossby wave speed, which is independent of frequency and wavenumber and hence will apply to a range of modes (and hence a clustering of energy at a particular angle in t-x space), with the shorter waves becoming more dispersive and thus producing a smaller signal in the radon transform. It is arguable whether this is really achieved (see a wide range of papers recently with Dudley Chelton, among others, arguing that the dominant speed tends to be more related to nonlinear, coherent eddies). Even in the purely linear limit, the radon transform clearly isn't the appropriate tool if interest lies in the dispersive part of the wave spectrum. In that case a two-dimensional Fourier method seems a good place to start, together with the idea of searching for a dispersion relation rather than simply a single speed. For example, see Zang and Wunsch (JPO 1999, doi: 10.1175/1520-0485(1999)029<2183:TODRFN>2.0.CO;2).

We are unsure of the relevance of this point to our study. The dispersive nature of the waves has nothing to do with the method of detection! Any examination of a widely used method requires the generation of a simulated signal in which the dominant phase speed is known (otherwise the method can’t be tested) and the only degree-of-freedom is the degree of dominance of this mode. This is precisely what we do in our study. Our examination does not address waves versus eddies and/or linear versus nonlinear features and/or dispersive versus non-dispersive waves. It’s just an assessment of the methods under conditions where the “answer” is known from the outset. Likewise, we don’t understand the reviewer’s reference to the Zang and Wunsch (1999) paper since we also examine the 2D-FFT method.

So there seems to me to be little added value in this contribution. The radon transform remains a good way to identify a dominant speed when there really is one. When there isn't, it is a poor method. There is nothing new or controversial about that.

Obviously, if one accepts the performance of existing methods as satisfactory there’s nothing that needs to be examine. We, however, feel that critical assessment of performance are at the heart of scientific quest.

Commonly used methods fail to detect known propagation speeds of simulated signals from time-longitude (Hovmöller) diagrams

Yair De-Leon[1], Nathan Paldor [1]

[1]Fredy and Nadine Herrmann Institute of Earth Sciences, The Hebrew University of Jerusalem, Edmond J. Safra Campus, Givat Ram, Jerusalem, 9190401, Israel

Correspondence to: Nathan Paldor (nathan.paldor@huji.ac.il)

Abstract. This work examines the accuracy and validity of two variants of Radon transform and two variants of the Two-Dimensional Fast Fourier Transform (2D FFT) that have been previously used for estimating the propagation speed of oceanic signals such as Sea Surface Height Anomalies (SSHA) derived from satellite borne altimeters based on time-longitude (Hovmöller) diagrams. The examination employs numerically simulated signals made up of 20 or 50 modes where one, randomly selected, mode has a larger amplitude than the uniform amplitude of the other modes. Since the dominant input mode is ab-initio known, we can clearly define "success" in detecting its phase/propagation speed. We show that all previously employed variants fail to detect the phase speed of the dominant input mode even when its amplitude is 5 times larger than all other modes and that they successfully detect the phase speed of the dominant input mode only when its amplitude is 10 times (or more) larger than the other modes. This requirement is an unrealistic limitation on oceanic observations such as SSHA. In addition, three of the variant methods “detect” a dominant mode even when all modes have the exact same amplitude. The accuracy with which the four methods identify a dominant input mode **decreases** with the increase in the number of modes in the signal. Our findings are relevant to the reliability of phase speed estimates of SSHA observations and the reported “too fast” phase speed of baroclinic Rossby waves in the ocean.

1 Introduction

Time-longitude (Hovmöller) diagrams at a given latitude of an oceanic variable, $\eta(x,t)$, that represents e.g. temperature, sea surface height, chlorophyll, etc. obtained for example by satellite observations are often used for estimating the propagation rate of the oceanic variable. The rate at which $\eta(x,t)$ propagates is determined by the inverse slopes of same-amplitude contours. These slopes are calculated by applying various methods, employed in image processing and detailed below in Sect. 2.2, to the raw data or to processed data (e.g. Polito and Liu, 2003 who separated the data into tiles of different periods). The methods examined here were used in many oceanic sub-areas such as: The propagation speed of Rossby waves using SSHA (e.g. Tulloch et al., 2009) or data other than SSHA (Belonenko et al., 2018; Xie et al., 2016); Nearshore wave dynamics (Almar et al., 2014); Eddy detection (Abernathey and Marshall, 2013; Oliveira and Polito, 2018) and Intraseasonal variability from mooring (Hu et al. 2018) to name a few.

De-Leon and Paldor (2017a) examined the accuracy of various methods in estimating the phase speed of waves by applying these methods to an artificially generated signal made of 3 sine functions (modes) with known phase speeds and amplitudes, compounded by large-amplitude random white noise. All methods have successfully filtered out the high amplitude white-noise from the 3-harmonic signal and accurately detected the main mode (some of them also detected the secondary modes). However, such a signal is too synthetic/ideal and cannot be compared to real oceanic observations that include tens, if not hundreds, of modes with different frequencies and propagation speeds and not just 3 modes compounded by white noise.

In this short study we simulate "oceanic observations" and examine whether the methods detect a single dominant propagation speed out of many (20 or 50) speeds. In Sect. 2 we provide details on the generation of "observed" η signal, the methods for evaluating the propagation speed of the signal and the tests we apply to the signals. The results are shown in Sect. 3 and discussed in Sect. 4.

2 "Data" and methods

2.1 Generating the simulated "observations"

The η signals (where η is any oceanic variable) used here are generated numerically by summing up N purely propagating sine functions (modes, hereafter) of the form $\sin(kx-\omega t)$ where k is the zonal wavenumber, x is longitude, t is time and $\omega=kC$ is the frequency (where C is the zonal propagation speed). The number of participating modes, N, is taken to be either 20 or 50 and N-1 of these modes have an amplitude of 1 while the amplitude of the additional N^{th}, randomly chosen, mode is either larger than or equal to 1. The sum of all N modes constitutes the η-signal which is analyzed by the methods described in 2.2.

The "spatial domain" (x) is chosen between "longitudes" 70-130° on a Cartesian grid with a 1/4° resolution, and the "time" (t) duration is 20 years (1044 weeks) with temporal resolution of one datum per week, similar to publicly distributed products by e.g. Aviso. The values of the propagation speeds, C, are uniformly distributed in the -18 to 0 cm s^{-1} range (i.e. each of the 20 or 50 modes is assigned a different propagation speed within that range), which is typical for baroclinic Rossby waves in the ocean (see e.g. Fig. 7 of Killworth et al., 1997; Barron et al., 2009). The values of the frequencies, ω, are selected randomly so that the period, $2\pi/\omega$, falls in the range between 5 and 200 weeks while the values of the zonal wavenumbers, k, equal ω/C. The resulting signal was low-pass filtered by applying a 5-week-running-average at each grid point to eliminate short term variations.

The η signal made up of the filtered signal (i.e. the sum of N pure sine waves) at a given latitude, is plotted as a function of longitude and time (Hovmöller diagram). When a single dominant mode exists that has a certain propagation speed the pattern on this diagram is a straight line whose slope is the inverse of the dominant propagation speed (since the abscissa is longitude and the ordinate is time). An example of a time-longitude diagram of an artificial signal is shown in Fig. 1a (for signal with dominant input mode's amplitude of 1.5) where the slope of the solid blue line corresponds to the propagation speed of the dominant input mode. The challenge is to estimate the dominant speeds using different methods and examine their success in detecting the propagation speed of the known dominant input mode. The methods examined here are detailed in the next subsection.

2.2 Methods for estimating the "observed" propagation speed

Four variants of methods have been employed for identifying the preferred direction of the same-amplitude contours on the Hovmöller diagram, each variant relates a certain measure of the power/intensity in a mode to its propagation speed. The first method is the Radon transform, used by e.g. Chelton and Schlax (1996); Chelton et al. (2003) and Tulloch et al. (2009) for analysing satellite observations of the ocean. In this method, one calculates the sum of the amplitudes along lines inclined at an angle θ and displaced a distance s from the origin. Then, the sum of squares of the values of these sums along all lines having the same angle is calculated and the angle at which this sum of squares is maximal, is the best estimate for the orientation of the lines on the image. The dominant propagation speed of the signal is then proportional to the tangent of this angle of maximum sum-of-squares. In the second method, which is a variant of the Radon transform, the variance of the amplitudes is calculated along every angle θ instead of the sum of amplitudes. This method was applied e.g. by Polito and Liu (2003 to local auto-correlation of segments of Hovmöller diagram) and Barron et al. (2009). Another, independent, method commonly used (e.g. Zang and Wunsch, 1999; Osychny and Cornillon, 2004) is the two-dimensional Fast Fourier Transform (2D FFT). An example of (ω, k) diagram, obtained by applying 2D FFT to the signal of Fig. 1a is shown in Fig. 1b. Here we use two variants of the 2D FFT method: In the first variant one sweeps over the 2D FFT spectra to find the direction in (ω, k) plane with maximum "energy" (this is the third method) while in the second variant one finds the maximal amplitude of the 2D FFT (i.e. one of the bright points in Fig. 1b) and calculates the ratio ω/k where ω and k are the frequency and zonal wavenumber of the maximal amplitude (this is the fourth method). Detailed description of these methods and the interpretation of observed signals are found in De-Leon and Paldor (2017a).

Each of the four variants of the methods can yield an estimate of the dominant propagation speed of a signal, based on the extremum of a graph that relates the calculated measure of a mode's intensity to its propagation speed. An estimation of the propagation speed based on a local extremum of this graph is accepted when this extremum is narrow and isolated compared to other local extrema. When the normalized amplitude (the term normalized amplitudes is used for the calculated amplitudes divided by the maximal amplitude in the domain) of a distinct peak is 1 while the (normalized) amplitudes of all other peaks are smaller than 0.8, this mode is considered the dominant mode. In the variance method, where the extrema are minima, the dominant mode is accepted when its amplitude is 0.0 while the normalized amplitudes of all other minima are larger than 0.2. The results shown in Fig. 2 demonstrate the emergence of a “rejected” peak that does not differ significantly from other peaks (2d) and "accepted" peaks whose intensities are significantly larger than those of other peaks (2a, 2c) or "accepted" trough that is significantly smaller than the other troughs (2b).

2.3 Examining the accuracy of dominant mode detection

Two types of tests are applied to these “observations” to examine the accuracy of the various methods in assessing the existence of a dominant propagation speed (i.e. mode) in the signal.

The first is a true-positive/false-negative test in which there is a dominant mode in the “observed” signal and a given method indicates whether this dominant mode exists (true-positive; TP) or not (false-negative; FN). In our case, one of the sine functions (this is the dominant input mode) is chosen randomly and its amplitude is set to be larger than 1. We check for each method if (at all) it identifies a dominant mode and if so, if it matches the propagation speed of this (larger amplitude) input mode. We divide the interval of propagation speeds into N (=20 or 50) bins of equi-distant values and the determination of the success of the methods in identifying a dominant mode is as follows: if the dominant mode found by the method falls in the expected bin of the dominant input mode – we score it by 1 ("TP"). If it is found in one of its next neighbours, it is scored by 1/2. A score of 0 (“FN”) is assigned when the method cannot find any dominant mode and when it detects a dominant mode more than 1 bin away from the correct bin. For each of 5 values of dominant mode's amplitudes: 1.5, 2, 2.5, 5 and 10 and for 2 values of N (20 or 50) we repeat this procedure 50 times (i.e. for 50 different signals), sum up the scores and calculate the percentage of success in identifying the dominant input mode in the signals by TP/(TP+FN)*100. Since this choice of scoring (1, 1/2, 0) is arbitrary, we also considered an alternative arbitrary choice for scoring: 1 if the dominant mode falls in the expected bin of the dominant input mode; 2/3 in one of its nearest neighbours ; 1/3 in one of its next to nearest neighbours and 0 otherwise.

The second is a false-positive/true-negative test in which no dominant mode exists in the "observed" signal and a given method indicates that there **exists** a dominant mode (false-positive; FP) or not (true-negative; TN). In our case, this is done by generating a signal in which all modes have identical amplitudes (=1) and checking whether a method erroneously detects a certain propagation speed as dominant. If a dominant mode is detected, we score it by 1 ("FP"), if a peak is detected but is too wide we score it by 1/2 and if there is no dominant mode (i.e. no distinct peak or more than one peak) we score it by 0 ("TN"). We repeat this procedure 50 times for each of N=20 or N=50, sum up the scores and calculate the percentage of erroneous detection of dominant mode in the signals by FP/(FP+TN)*100.

3 Results

An example of false determination of the dominant mode is shown in Fig. 2 for the signal shown in Fig. 1a. Figure 2a shows the distribution of the sum-of-squares of the Radon transform versus C (black markers), normalized such that the maximum value equals 1. Also plotted are the dashed black vertical lines located at the N values of the uniformly distributed propagation speeds, C, where the solid blue line is located at the C-value of the dominant input mode's propagation speed. These dashed black and solid blue vertical lines are also shown in panels (b)-(d) of Fig. 2. Clearly, the dominant propagation speed calculated by the Radon transform (where the black curve attains its maximum) does not match the propagation speed of the dominant input mode. Figure 2b shows the (normalized) mean of variances as a function of C (black markers), and here, too, the calculated propagation speed (the curve’s minimum point) does not agree with the dominant input mode's speed. Figure 2c shows the (normalized) distribution of the sum-of-squares of the spectral coefficients (2D FFT-amplitudes) along different ω/k lines (sweeping) as a function of C (black markers) where a distinct peak exists but it's located far from the dominant input mode's propagation speed. Figure 2d shows the 20 highest (normalized) 2D FFT amplitudes of the (ω, k) diagram of Fig. 1b. There are many peaks with no clear single maximum and the dominant input mode has one of the lowest amplitudes. For this signal, none of the methods identified correctly the dominant input mode.

The statistics of success of each method in detecting the dominant input mode for the TP/FN test is shown in Fig. 3 for dominant input mode's amplitude of 2.5, 5 and 10. The results for amplitudes of 1.5 and 2 are not shown as the success rate of all methods at these amplitudes is between 10% and 30% only. In each case we repeated the procedure 50 times (i.e. for 50 signals; note that there is no significant difference in the results if the number of repeats is changed to 25 or 100) for N=20 and then for N=50, summed the scores (1, 1/2 or 0) and calculated the percentage of success by TP/(TP+FN)*100. (The second scoring of 1, 2/3, 1/3, 0 yielded very similar numbers (up to 3%) so they are not presented here). The conclusions from these results are: 1) in order to identify the dominant input mode with more than 70% certainty, its amplitude should be larger than 5. 2) No method has clear advantage over the other methods. 3) Clearly, as N increases the dominant mode's amplitude has to increase, too, for a successful identification (so as to ensure that the ratio between the dominant mode's amplitude and the sum of all amplitudes is similar for different values of N since, e.g., 2.5/20>2.5/50). 4) The amplitude at which successful detection occurs decreases with the decrease in the ranges of propagation speeds and periods. Thus, for propagation speeds in the range of -10 to -2 cm s^{-1} and periods between 15 and 100 weeks, an amplitude of 5 is successfully detected in over 90% of the cases, while an amplitude of 2 yields poor results (results not shown).

The statistics of erroneous detection of a dominant mode (the FP/TN test where the amplitudes of all input modes equal 1 i.e. there is no dominant input mode) is shown in Fig. 4 for each of the methods (here again we have generated 50 signals for N=20 and for N=50 and calculated the percentage of erroneous detection by FP/(FP+TN)*100). The 2D FFT maxima method is the only method for which the percentage of error is smaller than 20% while other 3 methods err in at least 50% of the cases (i.e. they identify a single clear peak in one of the propagation speeds). As N increases this erroneous detection percentage decreases slightly in the 2 Radon variants but increases slightly in the 2D FFT sweeping method.

4 Discussion

None of the methods can identify a dominant input mode unless its amplitude is significantly larger than the others (by a factor larger than 5! in the present study's ranges of propagation speeds and periods) and most of them (except the 2D FFT maxima) erroneously detect a dominant mode when there is no such input mode. Though the 2D FFT maxima method does not falsely detect dominant mode when it does not exist, its performance in detecting dominant input mode when it exists is not satisfactory. For realistic signals of the ocean we don't know that there is a dominant mode with sufficiently large amplitude so none of the methods is reliable for estimating the propagation speed of e.g. Rossby waves.

When the values of ω and k are chosen in a range corresponding to the resolution limit and the Nyquist frequency, the success of 2D FFT in identifying the dominant input mode's propagation speed increases significantly, compared to the case where the values of C are determined in advance, ω is chosen randomly in a particular range and k is set as a result of ω/C so aliasing can occur. For that reason, even if the signal includes only one mode (i.e. one C), and both ω and k are chosen in the latter manner, there can be a wrong identification by the 2D FFT (but the Radon transform identifies it correctly). In the ocean we don't know ab-initio which wave numbers and frequencies exist so we cannot filter them out of the signal; hence aliasing can occur, and the percentage of success in detecting the real dominant mode is expected to decrease further.

The erroneous identification of the Radon and variance methods can be partially attributed to the non-linear relation between the angle θ and the propagation speed, C, which is proportional to $\tan(\theta)$ so the equi-distant values of C are converted to θ-values that are very close to one another. Figure 5 shows the distribution of the sum of squares of the Radon transform versus θ for the signal shown in Fig. 1a (while the distribution of the sum of squares of the Radon transform versus C for that signal is shown in Fig. 2a). It is clear from this figure that the peak is located in the vicinity of θ values corresponding to many C values. However, the performance of the Radon variants improves with the increase of the dominant input mode's amplitude, so the non-linear relation between the angle and propagation speed is not the only reason for the mismatch.

As N (the number of modes) increases (it is impossible to establish a-priori a bound on the number of modes in the ocean), the dominant input mode's amplitude should be larger in order to be separately identified from modes with similar characteristics. In addition, the width of the bins becomes narrower as N increases so fewer results can be evaluated as success. Also, in narrower ranges of propagation speeds and periods and for the same number of bins, all methods correctly detect the dominant input mode at lower threshold amplitudes (results not shown).

The weakness of the methods in identifying the dominant mode points to the difficulty in comparison between theories and observations of baroclinic Rossby waves in the ocean and this difficulty might explain the lack of "continuity" of propagation speed estimates between adjacent latitudes in one (or more) methods. It can also explain why a validation of the higher order trapped wave theory (where the β term is treated consistently) has been confirmed by observations only in the Indian Ocean south of Australia (De-Leon and Paldor, 2017b) and not in other parts of the world ocean. In contrast to the harmonic theory whose propagation speed estimates are always slower than the observed speeds, the trapped wave theory differs from observations sporadically (see Fig 5 of De-Leon and Paldor, 2017b).

Competing interests. The authors declare that they have no conflict of interest.

References

Abernathey, R. P., and Marshall, J.: Global surface eddy diffusivities derived from satellite altimetry, *J. Geophys. Res. Oceans*, **118**: 901– 916, doi:10.1002/jgrc.20066, 2013.

Almar, R., Rodrigo Cienfuegos, H. M., Bonneton, P., Tissier, M., and Ruessink,G.: On the use of the Radon Transform in studying nearshore wave dynamics, *Coastal Engineering*, **92**, 24-30, doi: 10.1016/j.coastaleng.2014.06.008, 2014.

Barron, C. N., Kara, A. B., and Jacobs, G. A.: Objective estimates of westward Rossby wave and eddy propagation from sea surface height analyses. *J. Geophys. Res*. **114**: C03013, doi: 10.1029/2008JC005044, 2009.

Belonenko, T. V., Bashmachnikov, I. L. and Kubryakov A. A.: Horizontal advection of temperature and salinity by Rossby waves in the North Pacific, International *J. Rem. Sensing*, **39:8**, 2177-2188,DOI: 10.1080/01431161.2017.1420932, 2018.

Chelton, D. B. and Schlax, M. G.: Global observations of oceanic Rossby waves. *Science* **272**: 234-238, doi: 10.1126/science.272.5259.234, 1996.

Chelton, D. B., Schlax, M. G., Lyman, J. M., and Johnson, G.C.: Equatorially trapped Rossby waves in the presence of meridionally sheared baroclinic flow in the Pacific Ocean. *Prog. Oceanogr*. **56**: 323-380, doi: 10.1016/S0079-6611(03)00008-9, 2003.

De-Leon, Y., and Paldor, N.: An accurate procedure for estimating the phase speed of ocean waves from observations by satellite borne altimeters. *Acta Astronautica*, **137**, 504–511 http://dx.doi.org/10.1016/j.actaastro.2016.11.016, 2017a.

De-Leon, Y., and Paldor, N: Trapped planetary (Rossby) waves observed in the Indian Ocean by satellite borne altimeters. *Ocean Science*. **13**. 483-494, doi: 10.5194/os-13-483-2017, 2017b.

Hu, S., Sprintall, J., Guan, C., Sun, B., Wang, F., Yang, G., Jia, F., Wang, J., Hu D. and Chai, F.: Spatiotemporal features of intraseasonal oceanic variability in the Philippine Sea from mooring observations and numerical simulations. *J. Geophys. Res*.: *Oceans*, **123**, 4874– 4887. 2018. https://doi.org/10.1029/2017JC013653

Killworth, P. D., Chelton, D. B., and de Szoeke, R. A.: The speed of observed and theoretical long extratropical planetary waves. *J. Phys. Oceanogr*. **27**: 1946–1966, doi: 10.1175/1520-0485(1997)027<1946:TSOOAT>2.0.CO;2, 1997.

Oliveira, F.S.C., and Polito, P.S: Mesoscale eddy detection in satellite imagery of the oceans using the Radon transform, *Prog. in Oceanogr.*, **167**, 150-163, doi: 10.1016/j.pocean.2018.08.003, 2018.

Osychny, V., and Cornillon, P.: Properties of Rossby waves in the North Atlantic estimated from satellite data. *J. Phys. Oceanogr*. **34**: 61-76, doi: 10.1175/1520-0485(2004)034<0061:PORWIT>2.0.CO;2, 2004.

Polito, P. S., and Liu, W. T.: Global characterization of Rossby waves at several spectral bands. *J. Geophys. Res*. **108**(C1), 3018, doi:10.1029/2000JC000607, 2003.

Tulloch, R., Marshall, J., and Smith, K. S.: Interpretation of the propagation of surface altimetric observations in terms of planetary waves and geostrophic turbulence. *J. Geophys. Res*. **114**: C02005, doi: 10.1029/2008JC005055, 2009.

Xie, L., Zheng Q., Tian J., Zhang S., Feng. Y., and Li, X.: Cruise Observation of Rossby Waves with Finite Wavelengths Propagating from the Pacific to the South China Sea. *J. Phys. Oceanogr.*, **46**, 2897–2913,https://doi.org/10.1175/JPO-D-16-0071.1. 2016:

Zang, X., and Wunsch, C.: The observed dispersion relationship for North Pacific Rossby wave motions. *J. Phys. Oceanogr*. **29**: 2183 – 2190, doi: 10.1175/1520-0485(1999)029<2183:TODRFN>2.0.CO;2, 1999.

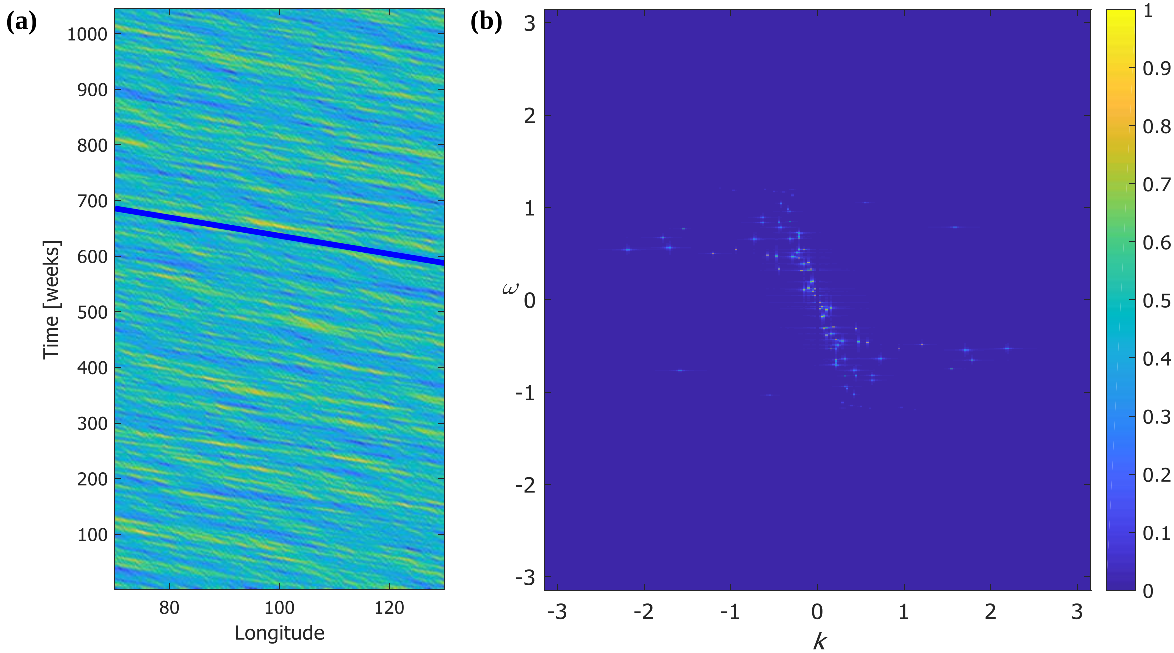

Figure 1: (a) An example of an artificial "observed" signal. (b) The associated (ω, k) diagram obtained by applying 2D FFT to the signal of panel (a). The solid blue line in panel (a) corresponds to the randomly chosen dominant input mode's propagation speed.

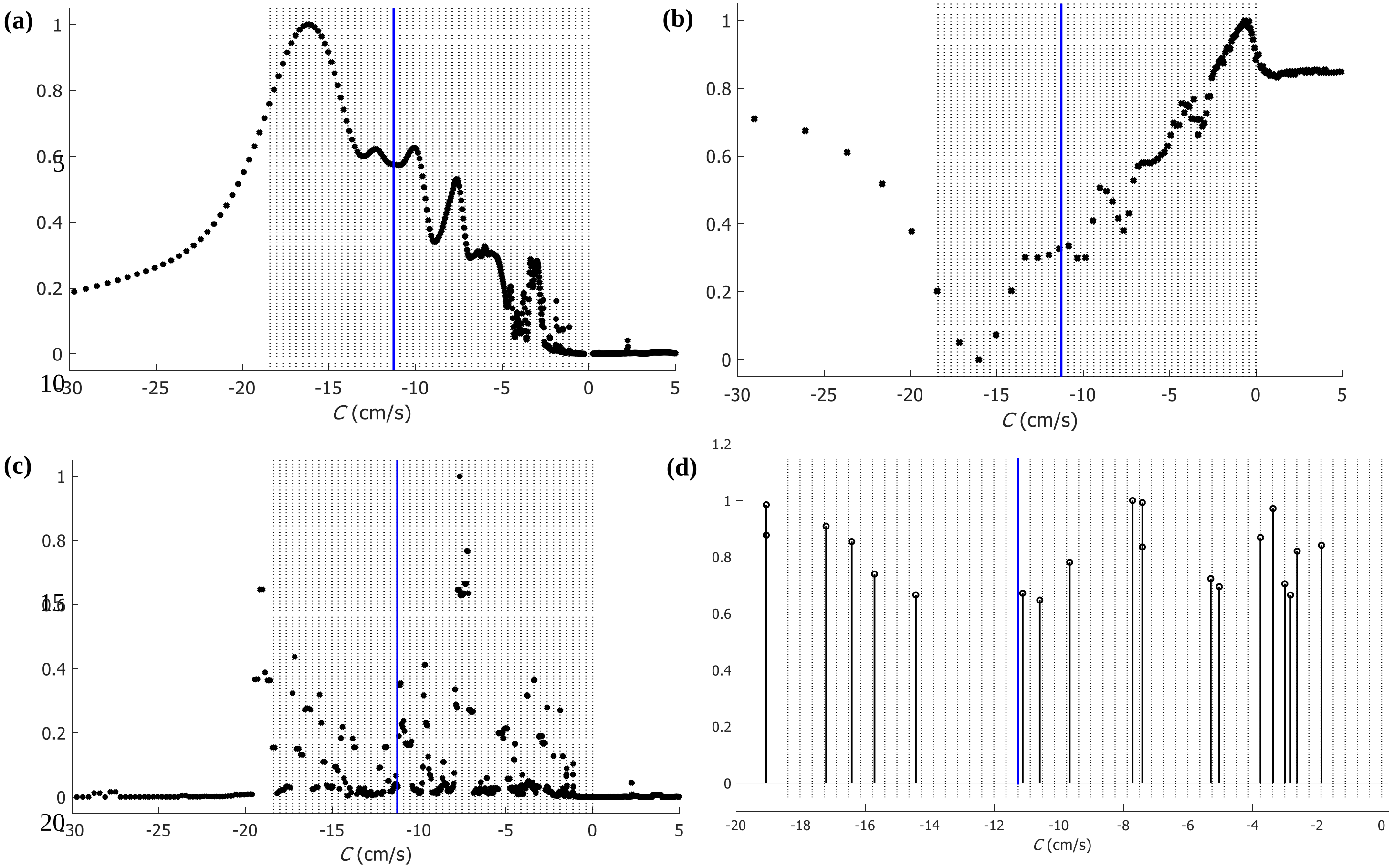

Figure 2: An application of the 4 methods to the artificially generated signal shown in Fig. 1a (panel a: Radon Transform, panel b: Variance, panel c: 2D FFT sweeping, panel d: 2D FFT maximal amplitude). Blue lines correspond to the dominant input mode propagation speed and dashed black lines correspond to the input modes' propagation speeds.

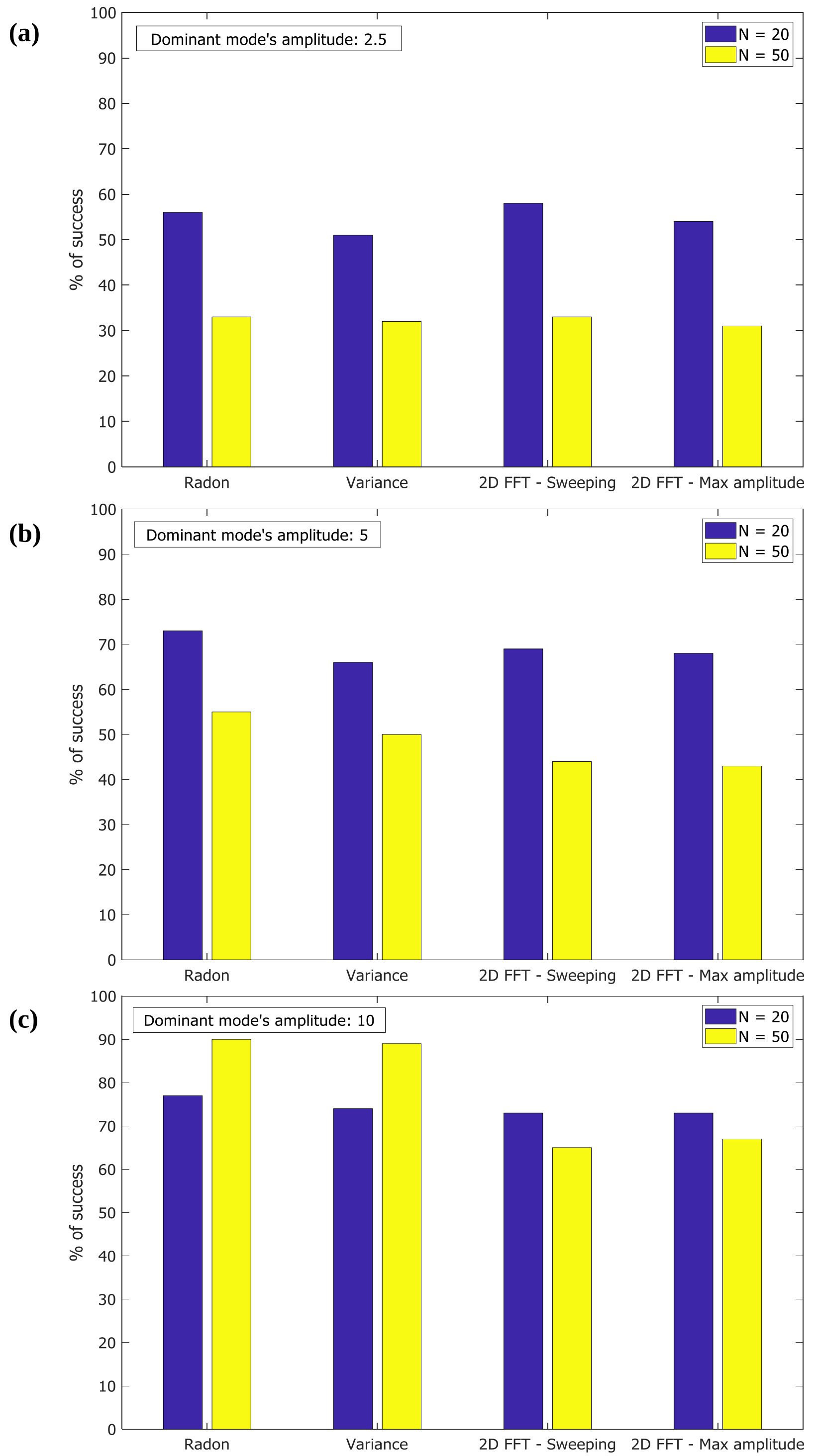

Figure 3: The percentage of success of each variant of the methods for dominant mode's amplitude of 2.5 (panel a), 5 (panel b) and 10 (panel c) for both N=20 and N=50.

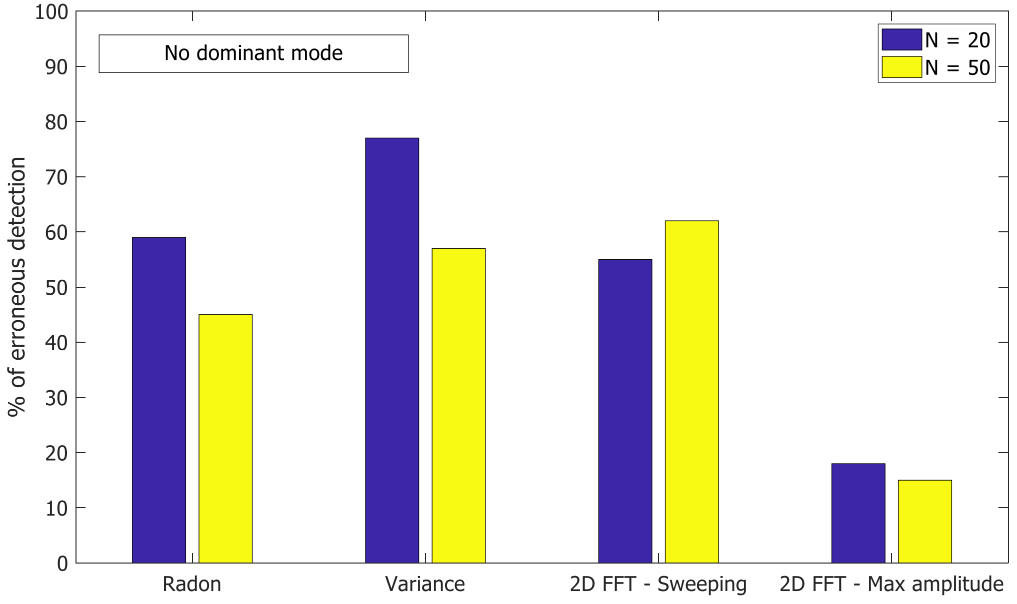

Figure 4: The percentage of error detection of each variant of the methods where there is no dominant input amplitude.

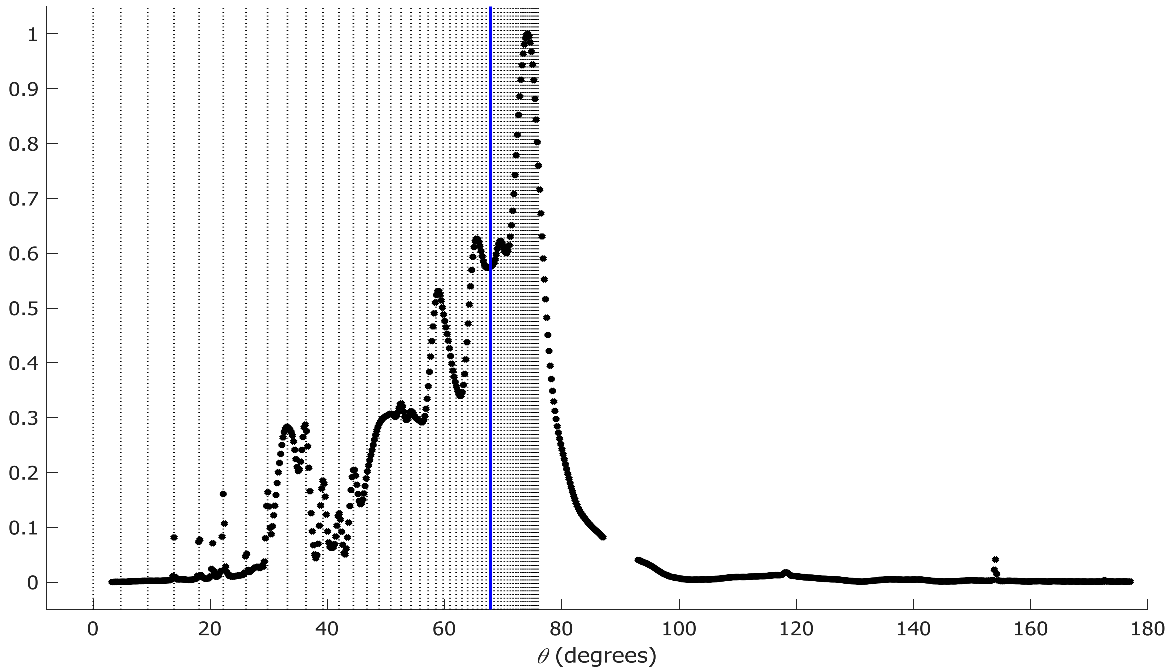

Figure 5: The distribution of the sum-of-squares of the Radon transform versus the Radon angle θ. Clearly, the distribution of the corresponding input propagation speeds (vertical dashed black lines) as a function of θ is not uniform due to the nonlinear relation between C and θ.